Transition Metal Ions in Microporous Crystalline Aluminophosphates: Isomorphous Substitution

Bert M. Weckhuysen,*[a] R. Ramachandra Rao,[a] Johan A. Martens,[a] and Robert A. Schoonheydt[a]

Keywords: Microporous crystalline aluminophosphates / Isomorphous substitution / Synthesis / Spectroscopy / Heterogeneous catalysis / Transition metal ion

Microporous crystalline metalloaluminophosphates (MeAPO-*n*) represent an important group of molecular sieves because of their potential catalytic and adsorptive properties. Many transition metal ions are claimed to incorporate in the framework of these molecular sieves. Here, the concept of isomorphous substitution, and the different indirect and direct tools available to verify this substitution process for Co, Cr, V, Fe and Mn are reviewed taking the $AlPO_4$-5 structure as an example. In addition, it will be shown that transition metal ions can be used as a probe to follow the hydrothermal synthesis process of microporous aluminophosphates.

[a] Centrum voor Oppervlaktechemie en Katalyse, Departement Interfasechemie, K.U. Leuven, Kardinaal Mercierlaan 92, B-3001 Heverlee (Leuven), Belgium
E-mail: Bert.Weckhuysen@agr.kuleuven.ac.be

Bert M. Weckhuysen was born in Aarschot, Belgium in 1968. In 1991 he received his M.S. degree from the Faculty of Agronomy and Applied Biological Sciences, Catholic University of Leuven, Belgium. From 1991 to 1995 he was employed as a doctoral student at the Center for Surface Chemistry and Catalysis under the supervision of Professor Robert A. Schoonheydt. There he gained experience in spectroscopic techniques, zeolite synthesis, catalyst design, and characterization. After obtaining his Ph.D. in Applied Biological Sciences in 1995, he has worked as a visiting research scientist with Professor Israel E. Wachs at the Zettlemoyer Center for Surface Studies of Lehigh University, USA. From 1996 to 1997 he has worked as a postdoc with Professor Jack H. Lunsford in the Chemistry Department of Texas A&M University, USA. Presently, he is a postdoctoral research fellow of the National Fund of Scientific Research at the Catholic University of Leuven. He is author of more than 50 scientific papers.

Ramachandra R. Rao was born in Kanigiri, India in 1968. In 1991 he received his M.S. degree from the A.P.S. University, Rewa, India. After obtaining his Ph.D. in Chemistry from the Osmania University, Hyderabad, India under the supervision of Dr. S. J. Kulkarni in 1996, he moved to the Catholic University of Leuven, Belgium. Presently, he is a postdoctoral fellow at the Department of Interphase Chemistry. His research interests are in the synthesis, characterization and applications of zeolite-based materials. He has authored more than 15 scientific publications.

Johan A. Martens was born in Jette, Belgium in 1958. He obtained his Ph.D. in Applied Biological Sciences at the Catholic University of Leuven, Belgium in 1985. After a research career at the National Fund of Scientific Research, he became full professor in environmental catalysis at the Department of Interphase Chemistry of the Catholic University of Leuven. His teaching assignments are in the fields of "Synthesis of the highly divided solids", "Adsorption" and "Catalysts, adsorbents and colloids for industry and environment". He is author of the book "Synthesis of high-silica aluminosilicate zeolites", editor of two conference proceedings and has published 120 scientific papers. In 1995, he was granted the Exxon Chemical Biannual Science and Engineering Award, for "pioneering research in heterogeneous catalysis for hydrocarbon and natural feedstocks". His current research themes are environmental catalysis, surface chemistry, sol-gel processes, synthesis of oxides, zeolites, adsorption and separation processes, petroleum refining and DeNOx processes.

Robert A. Schoonheydt received his M.S. degree in 1966 and his Ph.D. in 1970, both under the supervision of Professor Jan B. Uytterhoeven at the Catholic University of Leuven, Belgium. After one year as a postdoc with Professor Jack H. Lunsford in the Chemistry Department of Texas A&M University, USA, he returned to the Catholic University of Leuven as a National Fund of Scientific Researchresearcher. He became full professor in 1989. His teaching responsibilities include physical chemistry, analytical chemistry, and general thermodynamics for engineering students at the Faculty of Agricultural and Applied Biological Sciences. His research is concentrated in three areas: (1) spectroscopy and chemistry of surface transition metal ions; (2) molecular organization on clay surfaces, and (3) theoretical modeling of molecule-surface interactions. He has authored more than 170 scientific papers, and is the editor of the book "Developments in the theory of chemical reactivity and heterogeneous catalysis". Presently, he is secretary-general of AIPEA and dean of the Faculty of Agricultural and Applied Biological Sciences. He also serves on the editorial board of Microporous and Mesoporous Materials, Applied Clay Science and European Journal of Inorganic Chemistry.

MICROREVIEWS: This feature introduces the readers to the authors' research through a concise overview of the selected topic. Reference to important work from others in the field is included.

  1434–1948/99/0404–0565 $ 17.50+.50/0

Contents

1. Introduction

Material scientists usually subdivide the family of microporous crystalline oxides into silicate-based and phosphate-based materials[1] (Figure 1). Although this distinction has a historical origin because phosphate-based molecular sieves have been discovered after their silicate-based counterparts, it is often very arbitrary, as some molecular sieves contain both silicon and phosphorus; i.e., the silicoaluminophosphates (SAPO′s). In addition, two other classes of materials recently emerged, which includes the family of e.g. octahedral molecular sieves.

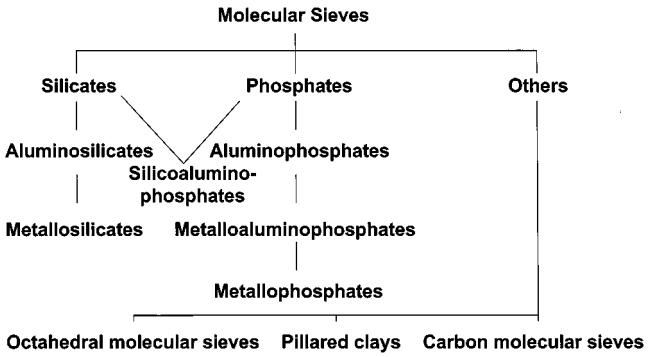

Figure 1. Molecular sieves can be split into three main families, the silicate-based materials containing the aluminosilicates or zeolites and the metallosilicates; the phosphate-based materials containing the aluminophosphates, silicoaluminophosphates, metalloaluminophosphates, and metallophosphates; and finally a remaining group of materials, such as the octahedral molecular sieves

Aluminophosphates consist of tetrahedra of Al^{3+} and P^{5+}, which are corner-sharing an oxygen atom, and building up a three-dimensional framework with channels and/or pores of molecular dimensions.[2,3] This is schematically illustrated in Figure 2. A well-known example is $AlPO_4$-5 (Figure 3), which has one-dimensional channels with 12-ring apertures of 7.3 Å diameter. The acronym $AlPO_4$-*n* is usually used for denoting the different framework structures, and actually more than 35 different topologies of $AlPO_4$-*n* materials are known in the literature.[1−3] All these materials are crystallized from aqueous or non-aqueous solutions at temperatures up to 473 K in the presence of organic structure-directing agents, called templates. Since the first publication on microporous crystalline aluminophosphates in 1982,[4] these materials have attracted a lot of attention mainly because of the promising catalytic and adsorptive properties. Recently, the family of phosphate-based molecular sieves has been further expanded towards mesoporous materials with channel dimensions up to 50 Å.[5]

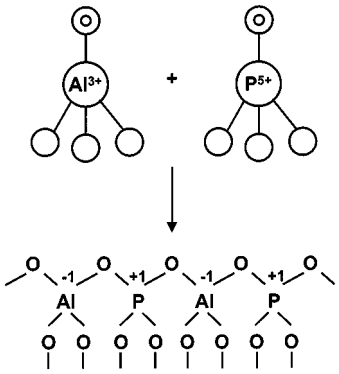

Figure 2. Assembly of a microporous aluminophosphate material (after ref.[1])

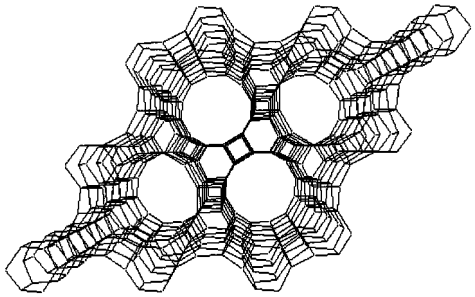

Figure 3. Pictorial representation of the $AlPO_4$-5 structure

In topological models of $AlPO_4$-*n* materials, Al^{3+} and P^{5+} are mostly considered to be both in tetrahedral coordination (Figure 2). This is generally true for dehydrated materials, but important framework distortions or coordination changes may occur in actual $AlPO_4$-*n* crystals in the presence of adsorbed molecules. Indeed, NMR experiments have revealed the formation of five- or six-fold coordinated Al^{3+} in $AlPO_4$-*n* (with n = 5, 11, 21, and 25) materials by interaction with water, ammonia, methanol and acetonitrile.[6] The adsorption of e.g. water may also result in the hydrolysis of Al−O−P bonds with the formation of hydroxy groups. Thus, interrupted frameworks can be formed, in which Al−O−P bonds are systematically missing. These aspects of crystal chemistry of microporous crystalline aluminophosphates seem to be essential in understanding the concept of isomorphous substitution.

Isomorphous substitution in dense oxides is defined as the replacement of an element in the crystalline framework by another element with similar cation radius and coordination requirements.[1c,1d] The concept of isomorphous substitution can be handled for molecular sieves as well, and is

very important because it may result in novel materials with special redox and catalytic properties. Although isomorphous substitution in $AlPO_4$-*n* materials is generally considered as a complex phenomenon, currently 17 elements are reported to replace Al^{3+} and/or P^{5+}; i.e., Be, B, Mg, Si, Ti, V, Cr, Mn, Fe, Co, Ni, Cu, Zn, Zr, Ge, Ga, and As.[1,7] Furthermore, the synthesis of multi-element phases containing up to six different elements has also been claimed.[12]

The only experimental limitation up to now was the substitution degree, which was set to about 38% of the Al^{3+} sites replaced by a particular transition metal ion (TMI).[8] However, very recently Stucky and co-workers were able to increase the substitution degree up to 90% by applying novel synthesis routes.[9] These results suggest that there exists no upper limit to the amount of a particular TMI incorporating in the framework of MeAPO-*n* materials. Indeed, the synthesis of microporous metallophosphates containing no aluminum is also reported in the literature. Some examples are UCSB-6GaCo, a microporous $Co_xGa_{1-x}PO_4$ material synthesized at the University of California at Santa Barbara,[9] DAF-2, a microporous $CoPO_4$ material discovered in the Davy Faraday Research Laboratory[10] and a microporous $ZnPO_4$.[11]

The aim of this review is to give an overview of the evidence currently available in the literature whether a TMI is isomorphously substituted in the framework of MeAPO-*n* materials or not. We will limit ourselves to CoAPO-5 (Co), CrAPO-5 (Cr), VAPO-5 (V), FAPO-5 (Fe), and MnAPO-5 (Mn) because of their well-documented literature. The paper starts with a brief review of the general concepts of isomorphous substitution. These concepts will then be applied to the different TMIs under study, and the obtained information will be compared with the available spectroscopic data. Both indirect and direct tools to verify isomorphous substitution will be discussed. In a third part, it will be shown that TMIs can be used as a probe to monitor the synthesis process of microporous crystalline aluminophosphates. In a final part, the application of microporous crystalline aluminophosphates in the field of heterogeneous catalysis will be briefly discussed. Special emphasis will be placed on possible leaching and mobility of the TMI. The review closes with some concluding remarks, and an outlook into the future.

2. Isomorphous Substitution

As mentioned above, isomorphous substitution in microporous crystalline aluminophosphates is complex, and two different substitution mechanisms can be envisaged for TMIs.[1] This is schematically illustrated in Figure 4. Substitution mechanism (SM) I involves the substitution of an Al atom for a TMI with valence +1 (Ia), +2 (Ib), or +3 (Ic), whereas SM II consists of the replacement of a P atom by a TMI with valence +4 (IIa) or +5 (IIb). Other types of substitutions not mentioned in Figure 4 seem to be very unlikely because they would lead either to positively charged frameworks or to a too high negative charge density. In the case of Si^{4+}, both P^{5+} and Al^{3+} are simultaneously replaced, and, as a consequence, silicon islands are formed in SAPO-5 materials. It is also clear from Figure 4 that SM Ia, Ib, and IIa lead to negatively charged frameworks, which must be balanced by an equivalent number of positively charged extra-framework species such as quaternary ammonium cations, protonated amines, hydroxonium ions or TMIs. On the other hand, SM Ic and IIb lead to electroneutral frameworks, and no charge balancing ions are involved. Finally, it is important to notice that TMI occurring in the synthesis medium under different oxidation states may be simultaneously incorporated according to different substitution mechanisms.

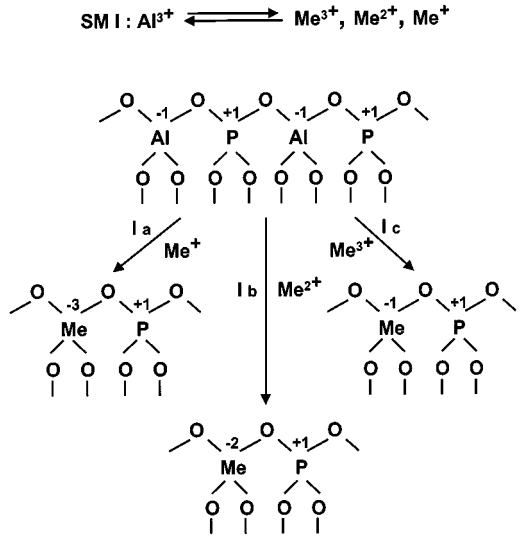

Figure 4A. Isomorphous substitution mechanism I (denoted as SM I) of $AlPO_4$-*n* molecular sieves (after ref.[1])

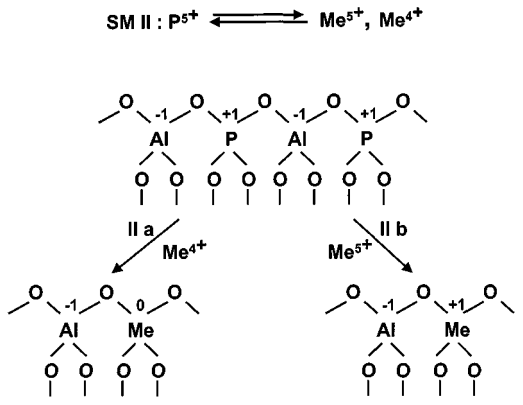

Figure 4B. Isomorphous substitution mechanism II (denoted as SM I) of $AlPO_4$-*n* molecular sieves (after ref.[1])

Four criteria are important for isomorphous substitution of a TMI in $AlPO_4$-5 materials:

(1) The formal charge and the ionic radius of the TMI to be incorporated. In the ionic bonding theory the limited ratios r_+/r_- for tetrahedral and octahedral coordination are

0.225 and 0.414, respectively, [with $r_- = r(O^{2-}) = 1.33$ Å and $r_+ = r$(cation) = 0.299 or 0.551 Å for tetrahedral or octahedral substitution, respectively]. According to Table 1, divalent transition metal ions are too large; trivalent cations are on the limit of tetrahedral coordination, while higher valency would in principle lead to isomorphous substitution.

(2) The solution chemistry of the TMI as a function of the pH of the synthesis gel. Here, it is crucial to avoid precipitation of insoluble transition metal hydroxides or oxides during the synthesis process because they may prevent that the TMI becomes available for isomorphous subsitution.

(3) The ligand field stabilization energy (LFSE) of the TMI. In the cases under study octahedral coordination is always the preferred one.

(4) The thermodynamic stability of the resulting microporous aluminophosphate framework.

Table 1. Ionic cation radii [Å] for different coordination geometries of P, Al, and transition metal ions

Cation	4	5	6	Cation	4	5	6
P^{5+}	0.17	–	–	Mn^{4+}	–	–	0.54
Al^{3+}	0.39	–	0.53	Mn^{3+}	–	0.58	0.65
Co^{2+}	0.57	–	0.74	Mn^{2+}	–	–	0.82
Co^{3+}	–	–	0.61				
Fe^{2+}	0.63	–	0.78				
Fe^{3+}	0.49	–	0.65	Cr^{6+}	0.30	–	–
V^{5+}	0.355	0.46	0.54	Cr^{5+}	0.35	–	–
V^{4+}	–	–	0.59	Cr^{3+}	–	–	0.615
V^{3+}	–	–	0.64	Cr^{2+}	–	–	0.82

Based on the cation radii and valence states it is then likely to assume that Co^{2+}, Fe^{2+}, and Fe^{3+} are substituting for Al^{3+} in the $AlPO_4$-5 framework according to SM Ib or Ic, whereas for example V^{5+} may replace P^{5+}. In any case, the possible incorporation of e.g. octahedrally coordinated Cr^{3+} and Mn^{2+} ions can only be explained by the flexibility of the aluminophosphate framework, and specific interactions with e.g. the organic template molecule. An additional explanation can be found in the unique possibility to increase the coordination number from four to five or six by interaction with additional ligands not being part of the framework; e.g., H_2O or OH groups, as was already discussed above for framework aluminum in $AlPO_4$-5 materials.[6] In addition, TMIs may also exist as oxides or extra-framework cations at the surface of the molecular sieves. Thus, the goal is then to develop direct and indirect tools which are able to verify isomorphous substitution.

3. Indirect Tools to Verify Isomorphous Substitution

The incorporation of TMIs into the framework of $AlPO_4$-5 materials would lead to an increase in unit cell volume of the crystal structure, all other factors remaining invariant (symmetry, etc.). This is expected because the radii of high-spin tetrahedral TMI, in a *T*-O matrix, is larger than that of Al^{3+} or P^{5+} (Table 1), and this expansion can be directly measured by X-ray diffraction techniques (XRD), according to

$$4/3\ [(h^2 + hk + k^2)/a^2] + l^2/c^2 = (4 \sin^2\theta)/\lambda^2$$

with *a* and *c*, the cell parameters of the unit cell of a hexagonal system; θ, the diffraction angle; and λ, the wavelength of the incident X-rays. An example of such a lattice expansion is shown for VAPO-5 materials in Figure 5.[12] However, such lattice expansions are not always observed, and no lattice expansions or even lattice contractions are reported in the literature for MeAPO-5 systems.[13] One of the explanations is that the amount of TMI is not sufficient to change the unit cell dimensions within the experimental error of the system.

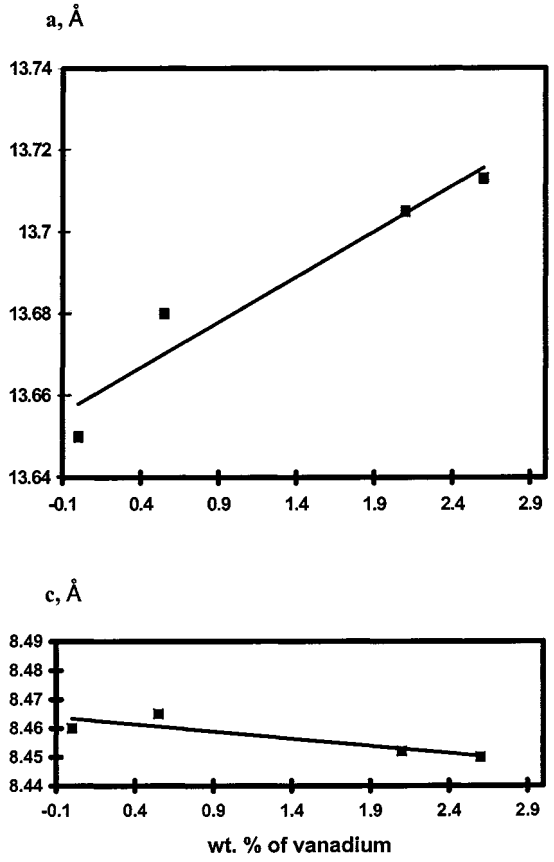

Figure 5. Lattice expansion as observed for VAPO-5 materials: variation of the *a* and *c* cell parameters as a function of the vanadium content (after ref.[12])

Isomorphous substitution can also be verified by chemical analysis. One expect then that the molar ratio of ([TMI] + [Al])/[P] (if the TMI is replacing Al) or ([TMI] + [P])/[Al] (if the TMI is replacing P) is equal to 1. Although this method is still very useful, it is very arbitrary and often inaccurate. Indeed, unreasonable values will be obtained if extra-framework TMI is present or if different substitution mechanisms simultaneously occur in the synthesis medium.

Another method to verify isomorphous substitution is by measuring the weight loss, associated with the burning of the template molecule. In the case of the template molecule Et_3NH^+, one can write the following combustion reaction:

$Et_3NH^+ + 11\ O_2 \rightarrow 6\ CO_2 + 8\ H_2O + NO_2$. It is then assumed that for every TMI^{n+} ($n = 2$) substituting for Al in the lattice, one template molecule is needed to compensate for the negative charge of the framework. It is important to notice that the combustion process of an occluded and positively charged template molecule usually occurs at a higher temperature than that of an adsorbed neutral template molecule.

The formation of extra-framework TMI can be indirectly probed by comparing the volume of intrachannel void space of MeAPO-5 and $AlPO_4$-5. Indeed, the generation of extra-framework species in channels and cavities would reduce the available void space of the $AlPO_4$-5 crystals.

Finally, if Me^{2+} (e.g., Co^{2+}, Fe^{2+}, and Mn^{2+}) substitute for Al^{3+}, one expects the formation of Brønsted acid sites in a concentration equal to that of Me^{2+}. The amount of Brønsted acid sites can be measured by performing TPD with e.g. a secondary amine, such as isopropylamine. Another interesting method is IR spectroscopy in conjunction with ammonia and acetonitrile as probe molecules. One of the problems here is to distinguish between the different forms of acidity (Lewis vs. Brønsted acidity).

The results of the application of these indirect measurements for isomorphous substitution to MeAPO-5 materials (with Me = Co, Cr, V, Fe, and Mn) are summarized in Table 2. It is clear that there is indirect evidence for the isomorphous substitution of Co^{2+}, $Fe^{2+/3+}$, and Mn^{2+} into the framework of $AlPO_4$-5 molecular sieves. Another problem with indirect methods, besides that they being indirect, is the lack of sensitivity. As a consequence, relatively high amounts of framework TMI are necessary to observe characteristic changes with the techniques mentioned.

4. Direct Tools to Verify Isomorphous Substitution

It can be concluded from the previous section that other more direct − preferably spectroscopic − techniques have to be called in to distinguish between framework and extra-framework TMI. Because each spectroscopic technique has its own sensitivity and application domain, a whole battery of complementary spectroscopic techniques has been applied to obtain detailed information of the coordination environment of TMI. Another disadvantage is the occurrence of complex and overlapping spectra, and chemometrical techniques have to be called in to obtain fingerprint spectra of framework and extra-framework TMI.

4.1. Cobalt

CoAPO-5 is probably the most studied MeAPO-*n* system ever. This can be easily explained by the fact that almost all scientists agree that Co^{2+} is substituting − at least partially − for Al^{3+} in the framework. This has been evidenced by applying a combination of DRS, ES, and EXAFS spectroscopies.

As mentioned above, the TMI content that can be incorporated into the $AlPO_4$-5 structure is still limited, and attempts to synthesize CoAPO-5 with high Co content usually lead to low-crystalline products contaminated with impurities.[15] An explanation for the failure in obtaining a pure CoAPO-5 phase from Co-rich gels can be the more favorable crystallization of other competing crystalline phases, such as the chabazite structure of CoAPO-34.[16,17] In addition, when attempting to incorporate large amounts of Co^{2+} in the framework, some of the Co^{2+} is present as octahedral Co^{2+}, clustered CoO and/or a $CoAl_2O_4$ phase.[18]

CoAPO-5 materials have been studied in detail by DRS spectroscopy, and an example of a set of DRS spectra is shown in Figure 6. The absorption bands for the blue, as-synthesized CoAPO-5 are typical for a perfect tetrahedron $[CoO_4]$ with two triplets centered at $\nu_2 = 6700\ cm^{-1}$ and $\nu_3 = 17300\ cm^{-1}$. This observation, together with the linear dependency of the band intensities with the Co^{2+} content are taken as proof of incorporation of Co^{2+} in the lattice. This is surprising because (1) the Co^{2+} radius of 0.57 Å is on the limit of tetrahedral and octahedral coordination and (2) the Co^{2+} radius is significantly larger than that of Al^{3+} (Table 1). As a consequence, a distortion of the $[CoO_4]$ tetrahedron is expected, and this strain is relieved in the lattice by interaction with adsorbed molecules in the 12-ring channels of the $AlPO_4$-5 structure.

This is proven by the DRS spectra taken after calcination in O_2 (Figure 6). A yellow-green sample is obtained with a distorted Co^{2+} species with two triplets centered at $\nu_2 = 5500\ cm^{-1}$ and $\nu_3 = 15150\ cm^{-1}$. These frequencies are indicative of a weaker ligand field, too. The distortion and strain of the zeolite lattice is reflected by the instability of the framework Co^{2+}. Indeed, part of the Co^{2+} is expelled from the lattice to give extra-framework pseudo-tetrahedral Co^{2+} ($\nu_2 = 5500$ and $\nu_3 = 16500\ cm^{-1}$) and octahedral Co^{2+} ($\nu_2 = 8100$ and $\nu_3 = 19550\ cm^{-1}$). A fraction of the Co remaining in the lattice is oxidized to high-spin tetrahedral Co^{3+} with its characteristic d-d transition at around

Table 2. Indirect criteria to verify isomorphous substitution of TMI in $AlPO_4$-5 molecular sieves

TMI	Lattice expansion	Chemical analysis	Template burning	Void space	Brønsted acidity
Co^{2+}	+	+	+	+	+/−
Cr^{3+}	nd	+/−	nd	nd	ne
V^{4+}	+/−	+/−	+	+	nd
$Fe^{2+/3+}$	+	+	nd	nd	−, ne (Fe^{3+})
Mn^{2+}	+	+	nd	nd	+

+: positive evidence; −: negative evidence; +/−: mixed opinions in the literature; nd: not determined; ne: not expected.

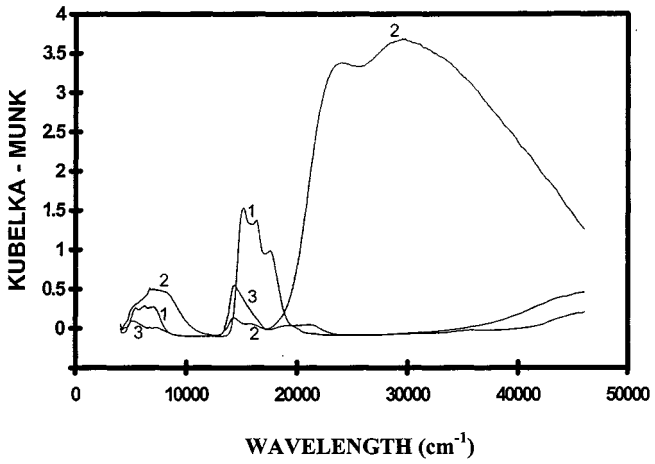

Figure 6. DRS spectra of CoAPO-5 materials as a function of the pretreatment: (1) in as-synthesized form; (b) after calcination overnight at 773 K and (3) after reduction with H_2 at 623 K (after ref.[16])

9000 cm^{-1}, and very intense $O \rightarrow Co^{3+}$ charge transfer transitions around 25000 and 31500 cm^{-1}.

The redox chemistry of Co is reversible. Co^{3+} is quantitatively reduced to Co^{2+} by H_2 at high temperatures, but also by CO, NO, methanol, acetone, and toluene.[16,19–25] The overall scheme of this reaction is given in Figure 7. Additional evidence comes from the observation of a weak OH stretching band at 3540 cm^{-1} after reduction and its disappearance upon oxidation. Whether the presence of a DRS spectrum of tetrahedral Co^{2+} is still a sufficient proof of lattice-substituted Co^{2+} is questionable. Indeed, one might envisage octahedral lattice Co^{2+} by analogy with Al^{3+}, or the presence of extra-framework Co oxides in different forms.

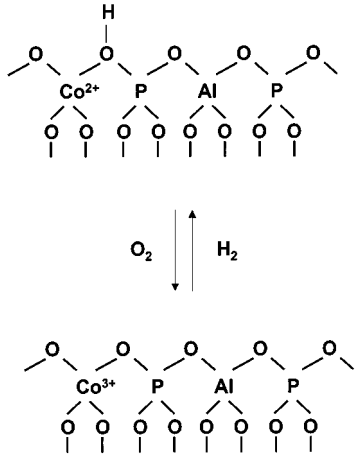

Figure 7. Schematic representation of the oxidation/reduction cycle of CoAPO-5 molecular sieves

Further evidence for the oxidation of Co^{2+} to Co^{3+} during calcination is found by ESR. A significantly reduced ESR signal in calcined CoAPO-5 was explained by a partial oxidation of Co^{2+} to the ESR invisible Co^{3+}.[20,21] Lee and Chon proved the oxidative abilities of CoAPO-5 with ESR by the formation of radicals upon interaction with alkenes.[26] However, this interpretation has been challenged by Kurshev et al.[27] These authors propose a distortion of the tetrahedral Co^{2+} environment to a dihedral symmetry resulting from the interaction of Co^{2+} with two O_2 molecules. Finally, Co K-edge EXAFS studies of CoAPO-5 recorded after synthesis and during calcination and reduction have only revealed small changes in bond lengths and coordination numbers of $Co^{2+/3+}$, suggesting an incomplete oxidation of the Co^{2+}.[28]

4.2. Chromium

The synthesis of CrAPO-5 molecular sieves has also been extensively studied in the literature, but the question remains if Cr^{3+} really substitutes for Al^{3+} in the framework, and to what extent.[29] Indeed, tetrahedral Cr^{3+} is difficult to obtain as evidenced by the scarcity of tetrahedral Cr^{3+} complexes and the absence of reported inorganic structures with tetrahedral Cr^{3+}.[30]

Figure 8 shows the DRS spectra of the green colored as-synthesized CrAPO-5 samples with increasing Cr content, which are characterized by two absorption bands at 15900 and 21800 cm^{-1}.[29][31] The intensities of both bands almost linearly increase with increasing Cr content, and they are assigned to the ν_1 and ν_2 transitions of octahedral Cr^{3+}. In addition, the 15900 cm^{-1} band has two weak shoulders, which are both spin-forbidden transitions. It is important to notice that during synthesis there is no indication for a transformation of Cr^{3+} (O_h) to Cr^{3+} (T_d). A similar conclusion can be made from dehydration experiments in vacuo of as-synthesized CrAPO-5 taking into account that dehydrated $AlPO_4$-5 does not possess octahedral Al^{3+} in the framework (vide supra). Thus, there is no unambiguous experimental evidence to propose an octahedral lattice Cr^{3+} species. Nevertheless, some authors have proposed such lattice Cr^{3+} (O_h) with two H_2O molecules completing its first coordination sphere:[32] $Cr^{3+}(O)_4(H_2O)_2$.

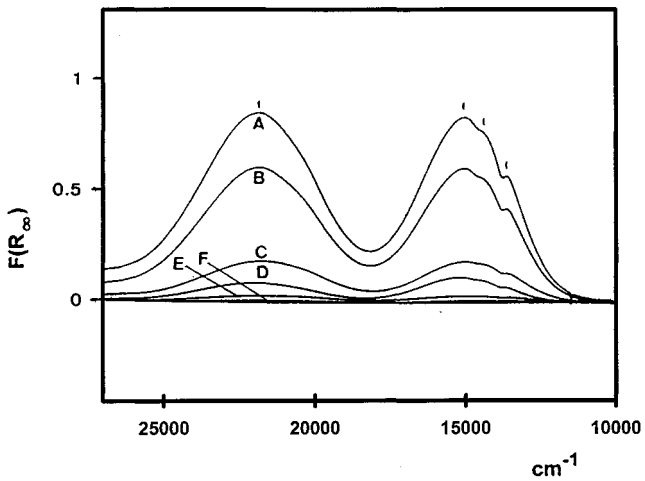

Figure 8. DRS spectra of as-synthesized CrAPO-5 materials as a function of the chromium content: 0.75 $R.(Cr_xAl_yP_z)O_4 \cdot 20\ H_2O$ with x = (A) 0.08; (B) 0.04; (C) 0.02; (D) 0.004; (E) 0.002, and (F) 0.0 (after ref.[29a])

Evidence for the presence of extra-framework Cr^{3+} comes from ESR experiments. The ESR spectra of as-synthesized CrAPO-5 are dominated by two characteristic signals: (1) a broad isotropic signal with $g = 2$ and (2) a rhombic signal with a positive lobe at $g_{eff} = 4.3$ and a weaker isotropic contribution at $g_{eff} = 2$. The zero-field parameters D and E are equal to 0.490 and 0.163 cm^{-1}, respectively. The former signal is typical for clustered Cr^{3+} in octahedral symmetry, which are most probably located as small oxidic particles at the outer surface or in the channels or pores of the molecules sieve. The latter signal is typical for Cr^{3+} in a strongly distorted environment, and because this signal is also observed for Cr^{3+} ions at the surface of amorphous supports (Al_2O_3, ...), one can assign it to distorted Cr^{3+} at the surface of $AlPO_4$-5.[33] By using other techniques, such as photoluminescence and single-crystal UV/Vis spectroscopy, others came to similar conclusions.[34−37]

Calcination in O_2 results in a color change from green to yellow-green. Both DRS and ESR spectroscopies indicate an incomplete oxidation of Cr^{3+} to Cr^{6+} with traces of Cr^{5+}. This suggests that some of the oxidic/isolated Cr^{3+} in the channels or pores of $AlPO_4$-5 resists oxidation. The formed Cr^{6+} is most probably attached to the surface of $AlPO_4$-5 as a chromate species with two extra-framework oxygen ions.[29,31]

4.3. Vanadium

VAPO-5 can be synthesized hydrothermally with different vanadium sources and template molecules, although the final oxidation state of vanadium largely depends on the vanadium source used.[12,13,38]. If V_2O_5 is used, some V^{5+} will be reduced to V^{4+} during hydrothermal synthesis, and a mixture of V^{4+} and V^{5+} is observed in the final solid products. The nature and properties of these vanadium sites are still a subject of debate. Up to now, it has not been proven unambiguously that vanadium really incorporates in the framework of $AlPO_4$-5 crystals, and the incorporation mechanism of $V^{4+/5+}$ is considered to be more complex than in the case of Co^{2+}.[39] This is not only due to the charge difference (proposal of substitution by SM II), but also because vanadium is prone to condensation reactions in solution, which lead to a variety of oligomeric species.

According to Montes et al.[13] and Jhung et al.[38] V^{4+} substitutes for P^{5+}, whereas Rigutto and van Bekkum[40] suggested the replacement of Al^{3+} by V^{4+}. Substitution of P^{5+} by V^{4+} is mainly proposed in view of a priori arguments such as the similarities between vanadium and phosphorus chemistry, and the existence of the mineral Schoderite, which contains both VO_4^{3-} and PO_4^{3-}.[41] The replacement of Al^{3+} by a $V{=}O^{2+}$ cation seems to be more convincing since the presence of the latter species is supported by spectroscopic evidence,[39,40,42] and no tetrahedral V^{4+} was ever detected by spectroscopic means. Indeed, combined DRS-ESR measurements have shown that V^{4+} is always present as a (pseudo-)octahedral species in VAPO-5.[39]

The above-mentioned models have in common that the vanadium sites are considered as monomeric. The key argument used for this assumption is that highly resolved ESR spectra are observed for as-synthesized VAPO-5 materials. However, clustered V^{4+} ions may be invisible due to line broadening as caused by spin-spin coupling of strongly interacting V^{4+} ions. If the vanadium ions tend to cluster one would expect that the amount of isolated V^{4+} ions as determined by quantitative ESR is lower than that expected from chemical analysis. This is indeed the case, and only 10% of the vanadium contributes to the ESR spectrum of VAPO-5.[39] Thus, V^{4+} is present as both isolated and clustered species, but it is uncertain whether both species substitute in the lattice. Finally, it is important to stress that two slightly different ESR signals are observed, which suggest the presence of two distinct V^{4+} ions, most probably located at defect sites.

Upon calcination in O_2, V^{4+} is almost completely oxidized to V^{5+} as evidenced by the weak V^{4+}-ESR signal and the observation of tetrahedrally coordinated V^{5+} (vanadate) by DRS and ^{51}V-NMR spectroscopies.[39,40,43] Reduction with CO or H_2 results in a partial regeneration of V^{4+}, and most probably lower oxidation states, such as V^{3+}, are formed.

4.4. Iron

FAPO-5 molecular sieves, discovered by Messina et al. in 1985,[44] can be synthesized using a variety of template molecules, typically amines or quaternary ammonium hydroxides, and either a Fe^{2+} or Fe^{3+} salt may be used as iron source. Regardless of the iron salt used, mostly both Fe^{2+} and Fe^{3+} are observed in the as-synthesized samples. Two reasons have to be invoked: (1) The oxidation of Fe^{2+} to Fe^{3+} in the initial synthesis gel. Indeed, by flushing the synthesis gel with nitrogen the oxidation to Fe^{3+} could be suppressed; and (2) the reduction of Fe^{3+} to Fe^{2+} by reaction with the amine template, according to $2\ Fe^{3+} + R_3N + H_2O \rightarrow 2\ Fe^{2+} + R_3NO + 2\ H^+$. The same reaction is responsible for the reduction of V^{5+} to V^{4+} during hydrothermal synthesis (vide supra). At low metal content, more than 90% of the iron is reduced, and with increasing iron content, the amount of reduced iron decreases only slowly. The reduction of Fe^{3+} can only be minimized by hydrothermal synthesis at lower temperature using e.g. tetraethylammonium hydroxide as template.

Several papers have appeared in the literature on the spectroscopic characterization of FAPO-5 molecular sieves.[45−55] The main techniques used were DRS, ESR, XPS, and Mössbauer spectroscopy. Especially ESR and Mössbauer spectroscopy seem to be very powerful, although their spectral interpretation is still a matter of debate.

As-synthesized FAPO-5 samples are characterized by a weak absorption at 23500 cm^{-1}, and an intense shoulder at around 26500 cm^{-1} in DRS. The former band is the spin-forbidden transition ν_3 of high-spin Fe^{3+} in tetrahedral coordination, while the latter is a charge-transfer transition of the type $O{\rightarrow}Fe^{3+}$.[46] It is assumed that the band at 23500

cm^{-1} is typical for Fe^{3+} in framework positions. No absorption bands of Fe^{2+} are detected. After calcination in O_2, the material turned from white to off-white, and the corresponding spectrum has characteristic absorption bands at 20800, 23000, 24400, and 26500 cm^{-1}. The transitions at 20800 and 23000 cm^{-1} are assigned to the spin-forbidden transitions ν_1 and ν_2, respectively, of high-spin Fe^{3+} in tetrahedral coordination.[46] Reduction with H_2 does not result in any spectral changes.

The co-existence of Fe^{2+} and Fe^{3+} in as-synthesized samples was unambiguously revealed by XPS. The binding energies of $Fe2p_{3/2}$ at 712.3 and 708.4 eV are assigned to framework Fe^{3+} and Fe^{2+}, respectively, while the presence of non-framework Fe^{3+} was evidenced by the $Fe2p_{3/2}$ peak at 710.5 eV. Calcination results in a total oxidation of Fe^{2+} to Fe^{3+}, and as a consequence, the disappearance of the $Fe2p_{3/2}$ peak at 708.4 eV. More detailed information can be obtained by Mössbauer spectroscopy. Four characteristic quadrupole doublets are observed, which are assigned to framework $Fe^{3+}(T_d)$; extra-framework $Fe^{3+}(O_h)$; framework $Fe^{2+}(T_d)$ and extra-framework $Fe^{2+}(T_d)$, their relative amounts depending on the treatment condition and the preparation method. For example, Schubert et al. found that as-synthesized FAPO-5 contains about 70% of Fe^{3+} and 30% of Fe^{2+}, and the amount of Fe^{3+} gradually increases with increasing calcination temperature.[51b]

Finally, ESR spectroscopy has been used to characterize the state of Fe^{3+} in FAPO-5 materials, and an example of an X-band ESR spectrum is given in Figure 9. Five different ESR signals can be observed: $g_1 = 2.0$; $g_2 = 2.2-2.3$; $g_3 = 4.3$; $g_4 = 5.2$ and $g_5 = 8.4$.[45] The two most intense signals are g_1 and g_2, and their assignments are still controversial. The traditional assignment is that g_1 is due to extra-lattice oxidic Fe^{3+}, whereas g_2 is due to framework Fe^{3+}. The three other signals would then be due to extra-lattice Fe^{3+} in various forms, although no detailed assignments have been given up to now. In light of recent work of Goldfarb et al.,[50] g_1 is due to both framework and extra-framework Fe^{3+}, whereas g_2 is typical for Fe^{3+} in a distorted tetrahedral coordination at defect sites. Thus, ESR alone will not be able to discriminate between framework and extra-framework Fe^{3+}.

It is important to notice that the relative intensity of g_2 decreases with increasing Fe loading, suggesting that Fe^{3+} will first coordinate to defect sites of the $AlPO_4$-5 crystals, while at higher loading, Fe^{3+} will incorporate in the framework or is present as small oxide particles. Upon calcination, the five ESR signals remain visible, suggesting that Fe^{3+} is relatively stable in the FAPO-5 material. Reduction results in a relative increase of the intensity of the g_1 signal, which can be explained by the formation of oxidic Fe^{3+}, and thus a migration and clustering of iron.

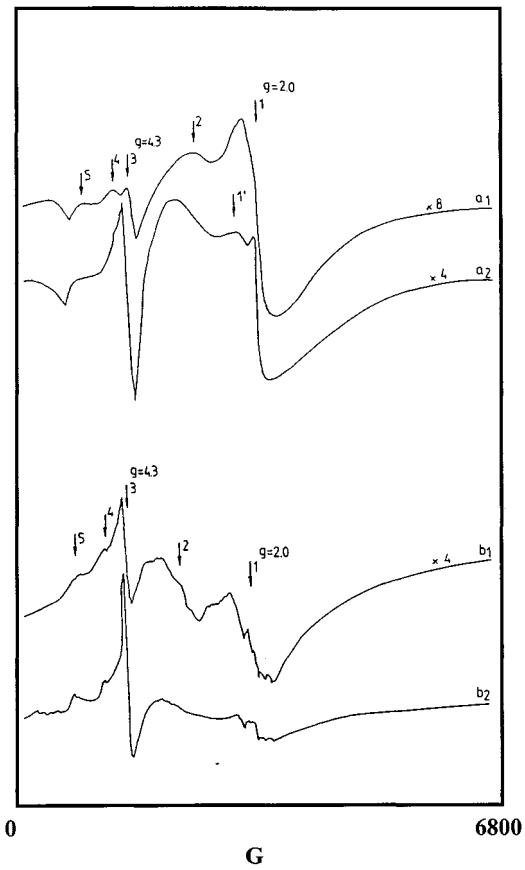

Figure 9. ESR spectra of FAPO-5 materials as a function of the pretreatment: (a) in as-synthesized form and (b) after calcination overnight at 773 K and helium flushing for 15 min at room temperature; the samples were measured at room temperature (1) and at 120 K (2) (after ref.[45])

4.5. Manganese

The evidence for the incorporation of Mn^{2+} into the framework of $AlPO_4$-5 is scarce. One of the reasons is the current discrepancy between the results obtained by indirect and direct tools to verify isomorphous substitution (Table 2). In addition, only ESR and its pulsed variant ESEEM have been applied to probe Mn^{2+} in $AlPO_4$-5 systems.[56–62] Thus, there is clearly a need to use other characterization techniques, such as DRS.

ESR spectroscopy of MnAPO-5 with a low manganese content shows six resolved hyperfine lines ($I = 5/2$) with a hyperfine coupling constant A of 90 G and a small zero-field splitting parameter D. Such ESR spectrum is typical for a slightly distorted octahedral Mn^{2+} species. In addition, ESEEM experiments showed that the isolated Mn^{2+} species interact through weak dipolar interactions with an average of six ^{31}P nuclei at a distance of 5 Å.[56][57] All these observations do not agree with a model in which Mn^{2+} is substituting for framework Al. As a consequence, it was concluded that the majority of Mn^{2+} in MnAPO-5 systems was present as extra-framework Mn^{2+}.

Dehydration of MnAPO-5 systems stimulates migration of the Mn^{2+} cations, resulting in an increase in spin exchange interaction, and only a single ESR line is observed. X-band and Q-band ESR spectra reveal that the 6-line hyperfine splitting is superimposed on a broader ESR signal, which has been assigned to transitions other than $-1/2 \rightarrow$

1/2 of Mn^{2+} with $I = 5/2$ or to another Mn^{2+} species by Levi et al.[57] Removal of water at increasing temperatures up to 400°C significantly broadens the hyperfine line and finally the resolution is completely lost and only one broad line is observed. Rehydration usually restores the 6-lines ESR spectrum of the hydrated MnAPO-5 sample completely.

The redox behavior of Mn^{2+} in MnAPO-5 materials has been investigated by Katzmarzyk et al.[59] Calcination in O_2 changes the color from white to deep blue or violet, and this color change is associated with an overall decrease of the Mn^{2+} ESR intensity. This decrease in signal intensity is attributed by the same authors to a partial oxidation of Mn^{2+} to the ESR inactive Mn^{3+}. Oxidation to Mn^{4+} can be ruled out because new ESR signals cannot be detected at the low measurement temperature (93 K). Addition of polar molecules, such as water and ammonia, causes a color change from blue to pink or even gray. Reduction of the sample with H_2 at temperatures below 450 K does not change the ESR spectrum, while after reduction at 475 K the ESR signal becomes narrower and more intense. A possible explanation is that reduction of Mn^{3+} to Mn^{2+} under these conditions leads to more ESR active spins.

Although the above-described ESR interpretations are challenged by several authors (e.g., the presence of cluster-like arrangements of the type $Mn^{2+}-O-P-O-Mn^{2+}$),[62,63] it is obvious that clear spectroscopic evidence of framework Mn^{2+} is still lacking in the literature.

5. Probing the Early Stages of the Crystallization Process

The synthesis of microporous crystalline aluminophosphates generally starts with a gel phase which is digested during synthesis at high temperatures. Several attempts have been made to elucidate the chemistry of this gel, and its hydrothermal digestion. A whole variety of characterization techniques, such as liquid-phase NMR, IR and Raman spectroscopy, have been applied. For example, the existence of aluminum phosphate entities in solution has been demonstrated by NMR.[64–66]

Another approach is to probe the coordination geometry of TMI during hydrothermal synthesis. Indeed if the TMI is incorporated in the lattice, the synthesis gel with octahedral $TMI(H_2O)_6^{n+}$ ions will be transformed during synthesis into a solid material containing tetrahedral framework and/or non-framework TMI. One way to study this synthesis process is to use spectroscopy to probe the TMI during synthesis. In this respect, DRS has been used to characterize the synthesis of CoAPO-5 from its early precursors to the formation of a crystalline phase.[67–69] This is possible because: (1) Co^{2+} is, as discussed above, relatively easily incorporated in the $AlPO_4$-5 framework during hydrothermal synthesis, and a distinction between tetrahedral and octahedral Co^{2+} can be made; (2) the DRS spectra have excellent quality; and (3) the DRS technique is applicable to both wet gels and dried solids, amorphous and crystalline as well.

Figure 10 shows the XRD and DRS intensities of the solid materials versus synthesis time. The DRS intensities of tetrahedral Co^{2+} increase concomitantly with the XRD intensities. Thus, as crystallization proceeds, Co^{2+} is incorporated in the structure. In the nucleation stage of the synthesis, the nuclei are too small to be detected by XRD, and DRS can then be used to probe the coordination of Co^{2+}. This is illustrated in Figure 11, where the DRS spectra of four distinct gel stages as a function of synthesis time are given.

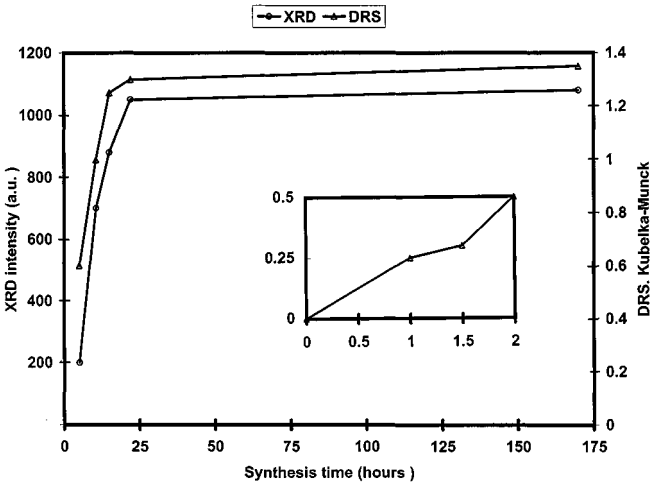

Figure 10. XRD and DRS intensities of the solid materials versus the synthesis time for CoAPO-5 materials (after ref.[67])

These gels were isolated from the autoclaves, and measured at room temperature. S_1 is the hydration-gelation phase, and nucleation has not yet started. Co^{2+} is octahedrally coordinated and not yet incorporated. It can be washed off by centrifugation. The DRS spectrum of gel S_2 consists of a weak triplet of tetrahedral Co^{2+}, superimposed on a broad band of (pseudo-)octahedral Co^{2+}. The latter is interpreted as cobalt with two water molecules in the first coordination sphere; i.e., $[CoO_4(H_2O)_2]$ taken up in the solid gel. Stage 3, which is attained after two hours of synthesis, is characterized by a dramatic increase of the band intensities of tetrahedral Co^{2+} at the expense of octahedral Co^{2+}. This means that Co^{2+} is being taken up by the CoAPO-5 material as $Co(OP)_4$. Further evidence for this transformation process comes from the decrease of the water bands in the NIR region. In stage S_4, the sample contains no water peak, indicating a full transformation of the gel into a crystalline phase. The peaks of tetrahedral cobalt are very intense and well resolved, which is indicative for Co^{2+} in identical crystallographic sites. The overall picture of the uptake of Co^{2+} can then schematically be shown as:

$$Co(H_2O)_6^{2+}\ \text{(liquid phase)} \rightarrow [CoO_4(H_2O)_6]\ \text{(gel phase)} \rightarrow [CoO_4]\ \text{(crystalline)}$$

This scheme is valid for CoAPO-5, but not for all structure types. Thus, CoAPO-34 synthesis is favoured at high template and Co contents; i.e., less water. This means that

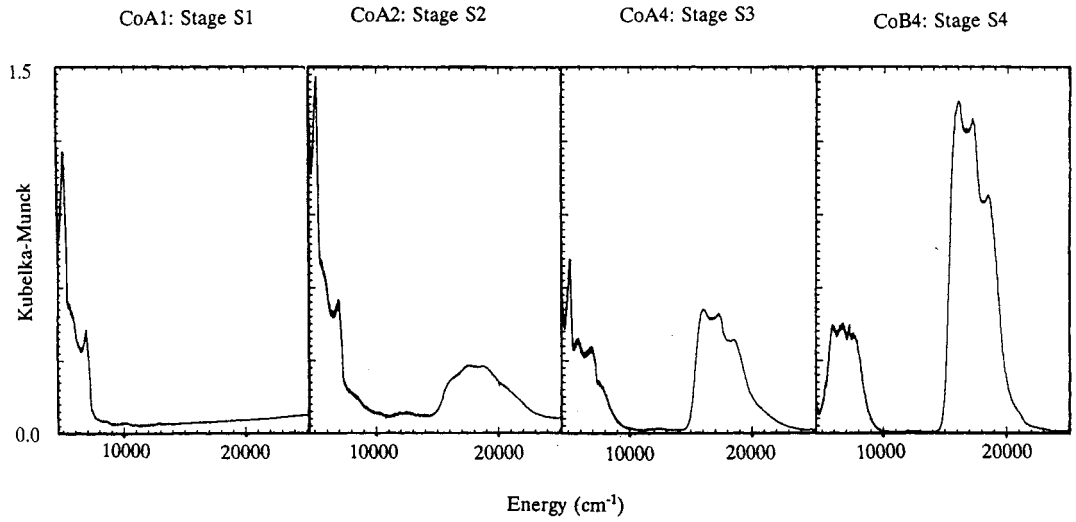

Figure 11. Four distinct gel stages for the synthesis of CoAPO-5, as recorded by DRS (after ref.[67])

upon interaction with the gel phase Co^{2+} is immediately transformed into a tetrahedral species:

$$Co(H_2O)_6^{2+}\ (\text{liquid phase}) \rightarrow [CoO_4]\ (\text{gel}) \rightarrow [CoO_4]\ (\text{crystal})$$

One observes that the template does not intervene directly in both schemes, but through its pH-regulating role it certainly influences indirectly the chemistry going on in the synthesis mixture.

6. Heterogeneous Catalysis

As mentioned above, MeAPO-5 molecular sieves have been explored as promising heterogeneous catalysts for both liquid-phase and gas-phase reactions. Their applications have been recently reviewed by Bellussi and Rigutto[70] and Arends et al.[71] Rather than summarizing the main results described, we would like to focus on the potential problems associated with their use in catalytic applications.

The catalytic activity of MeAPO-5 materials originates from the (co-)presence of Brønsted acid sites and/or redox centers, and thus in principle both acid- and redox-catalyzed reactions can be performed. Indeed, the activation of e.g. CoAPO-5 involves the calcination to remove template molecules. Simultaneously, part of the lattice TMI is oxidized to higher oxidation states (vide supra):

$$\text{CoAPO-5-}(Et)_3NH^+ \rightarrow (Co^{2+}{}_x,Co^{3+})H_x\text{-APO-5}$$

Protons are necessary for charge balance, and thus two catalytic functions are formed (Figure 7). If both Co^{2+} and Co^{3+} are in the lattice, they are expected to be in high-spin and in tetrahedral coordination. Redox catalysis requires free coordination sites, and this is impossible in such an ideal situation. Therefore, such type of catalysis can only be explained by (1) the presence of less than four lattice oxygen atoms around the TMI; (2) the lattice oxygen atoms, which are indirectly involved in redox chemistry or (3) the presence of extra-lattice TMI.

In addition, shape selectivity can be introduced in these molecular sieves because reactive substrates with a kinetic diameter larger than the pore size of the molecular sieve cannot react, whereas the reaction with a smaller molecule may proceed within the pore system. Another important advantage of such materials over their homogeneous counterparts is that the TMI is embedded in an inorganic microporous structure, which prevents or suppresses catalyst deactivation. Indeed, the most common deactivation mechanisms of homogeneous catalysts are the degradation of the (organic) ligands, and oligomerization of the active TMI.

Although the concept "reaction in micropores" generally leads to less catalyst deactivation, it is important to mention that other deactivation mechanisms may come into play; i.e., leaching of the active TMI and blocking of the microporous structure by a strong adsorption of reactants or products. Leaching of the active TMI is often severe, especially in the case of V and Cr, and several authors have attributed their observed catalytic activity solely to the presence of TMI leached in the reaction mixture.[72,73] In this respect, the composition of the reaction mixture is critical. Indeed, for CoAPO-5 molecular sieves it is proven that the molecular sieve dissolves during the oxidation of organic compounds in strong alkaline medium. On the other hand, in a strong apolar solvent (e.g. cyclohexane) an extremely low concentration of Co could be detected in solution, and the autoxidation activity of CoAPO-5 could not be attributed to this dissolved cobalt.[72] Another striking observation was recently found by Haanepen et al.[73] They observed that the leaching process of VAPO-5 molecular sieves only occurred in the beginning of the catalytic reaction, and that the heterogeneous contribution steadily stopped due to a strong adsorption of organic molecules in the pore system of $AlPO_4$-5. Removal of the VAPO-5 material from the reaction mixture after a short reaction time showed an ongo-

ing reaction in the filtrate. Similar results were obtained for CrAPO-5 molecular sieves.[74] Surely, the most promising direction for heterogeneous catalysis seems to be gas-phase reactions.[75] In this respect, the oxidative dehydrogenation of alkanes has received the most attention, and both VAPO-5 and MnAPO-5 are efficient catalysts for this type of reaction.[12,76,77]

7. Concluding Remarks and Look into the Future

The chemistry of TMIs in microporous aluminium phosphates is complex. The synthesis conditions of the materials do not favour incorporation of TMI in the lattice. In addition, the size of the TMI with respect to that of Al or P is such that substitution introduces strain in the structure. The following conclusions can be drawn from this microreview:

(1) Even at low metal loading, TMIs seem to be present under different coordination geometries; i.e.:

(a) Truly isomorphous substituted TMI possessing a (pseudo-)tetrahedral coordination. This has been spectroscopically proven for Co^{2+}, and to a lesser extent for $Fe^{2+/3+}$. It is important to notice that the presence of framework TMI with a higher coordination number (5 or 6) cannot be excluded (e.g., Cr^{3+}). Indeed, NMR studies have clearly shown the presence of octahedrally coordinated Al^{3+} in the framework of $AlPO_4$-*n* materials.

(b) Defect sites, which originate from interrupted frameworks in which Al−O−P bonds are missing. It is anticipated that Co^{2+}, Cr^{3+}, V^{4+}, $Fe^{2+/3+}$, and Mn^{2+} may coordinate to these defects, which will give rise to a (pseudo-)octahedral coordination. In this respect, it is remarkable to see that the overall crystallinity of the MeAPO-5 materials decreases with increasing metal loading. This suggests a continuous creation of defect sites in the framework with increasing incorporation of TMI.

(c) Extra-framework transition metal oxides, which are most probably located at the outer surface or occluded within the micropores of the molecular sieve. Spectroscopic evidence is available that Cr_2O_3, Fe_2O_3, and V_2O_4 clusters are formed during the synthesis of MeAPO-5 materials.

(2) More advanced synthesis procedures have to be developed which selectively increase the amount of framework TMI. The synthesis of nanosized transition metal oxides within the micropores could be another scientific challenge because of their possible quantum size properties.

(3) Both indirect and direct criteria to evaluate isomorphous substitution have been established. It is obvious that positive evidence via indirect criteria is not sufficient to claim a truly isomorphous substituted TMI. There is clearly a need to develop more refined spectroscopic tools to discriminate between framework and extra-framework TMI.

(4) Co^{2+} can be used as a probe for the synthesis mechanisms of microporous aluminium phosphates. Other TMIs, for which there is still no direct spectroscopic proof of lattice substitution, cannot be used as synthesis probes. Another approach, the in situ spectroscopy, might be a useful additional tool to extend this research direction.

(5) Only for Co^{3+}/Co^{2+} in the lattice has a clear redox chemistry been achieved, not yet for the other TMIs. Whether this is indicative for no incorporation of Fe, V, Cr, Mn in the lattice has still to be proven.

(6) The creation of Brønsted acid sites and redox centers makes MeAPO-5 interesting heterogeneous catalysts. However, the careful choice of the catalytic conditions is of paramount importance for the development of a successful catalytic application. In this respect, gas-phase catalysis seems to be a promising new direction.

The authors anticipate that the above-described remarks are also applicable to the isomorphous substitution of TMI in other molecular sieves.

Acknowledgments

B. M.W. is a postdoctoral fellow of the Fonds voor Wetenschappelijk Onderzoek − Vlaanderen (F.W.O), while R. R. R is thankful for a junior postdoctoral fellowship of the K. U. Leuven. This work was financially supported by the Geconcerteerde Onderzoeksacties (G.O.A.) of the Flemish Government.

List of Abbreviations

$AlPO_4$-*n* = microporous crystalline aluminophosphate

DRS = diffuse reflectance spectroscopy

ESEEM = electron spin echo envelope modulation

ESR = electron spin resonance

EXAFS = extended X-ray absorption fine structure

IR = infrared

LFSE = ligand field stabilization energy

MeAPO-*n* = microporous crystalline aluminophosphate containing a transition metal ion, Me

NMR = nuclear magnetic resonance

TMI = transition metal ion

TPD = temperature programmed desorption

XPS = X-ray photoelectron spectroscopy

XRD = X-ray diffraction

[1] [1a] J. A. Martens, P. A. Jacobs, *Stud. Surf. Sci. Catal.* **1994**, *85*, 653. − [1b] J. A. Martens, P. A. Jacobs, in *Catalysis and Zeolites* (Eds.: J. Weitkamp, L. Puppe), Springer Verlag, Berlin, in press. − [1c] M. Tielen, M. Geelen, P. A. Jacobs, in *Proc. Int. Symp Zeolite Catal.* (Eds.: P. Fejes, D. Kallo), *Acta Phys. Chem. Szegediensis* **1985**, *0*, 11. − [1d] D. W. Breck, in *Zeolite Molecular Sieves*, J. Wiley, New York, **1974**, p. 320.

[2] [2a] E. M. Flanigen, R. L. Patton, S. T. Wilson, in *Innovation in Zeolite Materials Science* (Eds.: P. J. Grobet, W. J. Mortier, E. F. Vansant, G. Schulz-Ekloff), Elsevier Science Publishers, B. V., Amsterdam, **1988**, p. 13. − [2b] R. E. Morris, S. J. Weigel, *Chem. Soc. Rev.* **1997**, *26*, 309. − [2c] S. T. Wilson, B. M. Lok, C. A. Messina, T. R. Cannan, E. M. Flanigen, in *ACS Series 218*, American Chemical Society, Washington, **1983**, p. 79.

[3] S. T. Wilson, E. M. Flanigen, in *ACS Series 234*, American Chemical Society, Washington, DC, **1989**, p. 329.

[4] [4a] S. T. Wilson, B. M. Lok, C. A. Messina, T. R. Cannan, E.

M. Flanigen, *U. S. Patent* **1984**, 4,440,871. – [4b] S. T. Wilson, B. M. Lok, C. A. Messina, T. R. Cannan, E. M. Flanigen, *J. Am. Chem. Soc.* **1982**, *104*, 1146.
[5] [5a] P. Feng, Y. Xia, J. Feng, X. Bu, G. Stucky, *Chem. Commun.* **1997**, 949. – [5b] D. Zhao, Z. Luan, L. Kevan, *Chem. Commun.* **1997**, 1009. – [5c] B. Chakraborty, A. C. Pilikottil, S. Das, B. Viswanathan, *Chem. Commun.* **1997**, 911.
[6] [6a] M. P. J. Peeters, L. J. M. van de Ven, J. W. de Haan, J. H. C. van Hooff, *J. Phys. Chem.* **1993**, *97*, 8254. – [6b] M. P. J. Peeters, J. W. de Haan, L. J. M. van de Ven, J. H. C. van Hooff, *J. Chem. Soc., Chem. Commun.* **1992**, 1560. – [6c] M. P. J. Peeters, J. W. de Haan, L. J. M. van deVen, J. H. C. van Hooff, *J. Phys. Chem.* **1993**, *97*, 5363. – [5d] R. Jelinek, B. F. Chmelka, Y. Wu, P. J. Grandinetti, A. Pines, P. J. Barrie, J. Klinowski, *J. Am. Chem. Soc.* **1991**, *113*, 4097.
[7] [7a] S. T. Wilson, B. M. Lok, E. M. Flanigen, *U. S. Patent* **1982**, 4,310,440. – [7b] S. T. Wilson, E. M. Flanigen, *U. S. Patent* **1986**, 4,567,029.
[8] I. M. Bennes, B. K. Marcus, in *Innovation of Zeolite Materials Science* (Eds.: P. J. Grobet, W. J. Mortier, E. F. Vansant, G. Schulz-Ekloff), Elsevier Science Publishers, B. V., Amsterdam, **1988**, p. 269.
[9] [9a] P. Feng, X. Bu, G. D. Stucky, *Nature* **1997**, *388*, 735. – [9b] X. Bu, P. Feng, G. D. Stucky, *Science* **1997**, *278*, 2080. – [9c] M. Jacoby, *Chem. Eng. News* **1997**, September 1, p. 11.
[10] J. Chen, R. H. Jones, S. Natarajan, M. B. Hursthous, J. M. Thomas, *Angew. Chem.* **1994**, *106*, 667; *Angew. Chem. Int. Ed. Engl.* **1994**, *33*, 639.
[11] T. E. Gier, G. D. Stucky, *Nature* **1991**, *349*, 508.
[12] T. Blasco, P. Concepcion, J. M. Lopez Nieto, J. Perez-Pariente, *J. Catal.* **1995**, *152*, 1.
[13] C. Montes, M. E. Davis, B. Murray, M. Narayana, *J. Phys. Chem.* **1990**, *94*, 6431.
[14] [14a] G. Lischke, B. Parlitz, U. Lohse, E. Schreier, R. Fricke, *Appl. Catal. A: General* **1998**, *166*, 351. – [14b] U. Lohse, R. Bertram, K. Jancke, I. Kurzawski, B. Parlitz, E. Loffler, E. Schreier, *J. Chem. Soc., Faraday Trans.* **1995**, *91*, 1163. – [14c] N. J. Tapp, N. B. Milestone, D. M. Bibby, in *Innovation in Zeolite Materials Science*, Elsevier Science Publishers, B. V., Amsterdam, **1988**, p. 393.
[15] V. P. Shiralkar, C. H. Saldarriaga, J. O. Perez, A. Clearfield, M. Chen, R. G. Anthony, J. A. Donohue, *Zeolites* **1989**, *9*, 474.
[16] A. A. Verberckmoes, M. G. Uytterhoeven, R. A. Schoonheydt, *Zeolites* **1997**, *19*, 180.
[17] A. A. Verberckmoes, B. M. Weckhuysen, R. A. Schoonheydt, *Microporous Mesopor. Mater.* **1998**, *22*, 165.
[18] J. H. Ashley, P. C. H. Mitchell, *J. Chem. Soc. A* **1968**, 2861.
[19] R. A. Schoonheydt, R. De Vos, J. Pelgrims, H. Leeman, in *Zeolites: Facts, Figures, Future* (Eds.: P. A. Jacobs, R. A. Vansanten), Elsevier, Amsterdam, **1989**, p. 559.
[20] L. E. Iton, I. Choi, J. A. Desjardins, V. A. Maroni, *Zeolites* **1989**, *9*, 535.
[21] C. Montes, M. E. Davis, B. Murray, M. Narayana, *J. Phys. Chem.* **1990**, *94*, 6425.
[22] B. Kraushaar-Czarnetzki, W. G. M. Hoogervorst, R. R. Andréa, C. A. Emeis, W. H. J. Stork, *J. Chem. Soc., Faraday Trans.* **1991**, *87*, 891.
[23] M. P. J. Peeters, J. H. C. van Hooff, R. A. Sheldon, V. L. Zholobenko, L. M. Kustov, V. B. Kazansky, *Proc. 9th Internat. Zeolite Confer.* (Eds.: R. von Ballmoos, J. B. Higgens, M. M. J. Treacy), Butterworth-Heinemann, New York, **1992**, p. 651.
[24] J. W. Couves, G. Sankar, J. M. Thomas, J. Chen, Catlow, C. R. A;R. Xu, G. N. Greaves, *Proc. 9th Internat. Zeolite Confer.* (Eds.: R. von Ballmoos, J. B. Higgens, M. M. J. Treacy), Butterworth-Heinemann, New York, **1992**, p. 627.
[25] [25a] K. Nakashiro, Ono, Y. *Bull. Chem. Soc. Jpn.* **1993**, *66*, 9. – [25b] J. Jänchen, M. P. J. Peeters, J. H. M. C. vanWolput, J. P. Wolthuizen, J. H. C. van Hooff, U. Lohse, *J. Chem. Soc., Faraday Trans.* **1994**, *90*, 1033.
[26] Y. J. Lee, H. Chon, *J. Chem. Soc., Faraday Trans.* **1996**, *92*, 3453.
[27] V. Kurshev, L. Kevan, D. J. Parillo, C. Pereira, G. T. Kokotailo, R. J. Gorte, *J. Phys. Chem.* **1994**, *98*, 10160.
[28] P. A. Barrett, G. Sankar, C. R. A. Catlow, J. M. Thomas, *J. Phys. Chem.* **1996**, *100*, 8977.
[29] [29a] B. M. Weckhuysen, R. A. Schoonheydt, *Zeolites* **1994**, *14*, 360. – [29b] B. M. Weckhuysen, R. A. Schoonheydt, *Stud. Surf. Sci. Catal.* **1994**, *84*, 965.
[30] [30a] A. B. P. Lever, *Inorganic Electronic Spectroscopy*, 2nd ed., Elsevier, Amsterdam, **1984**. – [30b] D. Reinen, *Struct. Bond.* **1969**, *6*, 30.
[31] B. M. Weckhuysen, I. E. Wachs, R. A. Schoonheydt, *Chem. Rev.* **1996**, *96*, 3327.
[32] [32a] J. D. Chen, R. A. Sheldon, *J. Catal.* **1995**, *153*, 1. – [32b] J. D. Chen, J. Dakka, E. Neeleman, R. A. Sheldon, *J. Chem. Soc., Chem. Commun.* **1993**, 1379.
[33] B. M. Weckhuysen, R. A. Schoonheydt, F. E. Mabbs, D. Collison, *J. Chem. Soc., Faraday Trans.* **1996**, *92*, 2431.
[34] N. Rajic, D. Stojakovic, S. Hocevar, V. Kaucic, *Zeolites* **1993**, *13*, 384.
[35] D. Demuth, K. K. Unger, F. Schüth, G. D. Stucky, V. I. Srdanov, *Adv. Mater.* **1994**, *6*, 931.
[36] D. Demuth, K. K. Unger, F. Schüth, V. I. Srdanov, G. D. Stucky, *J. Phys. Chem.* **1995**, *99*, 479.
[37] S. Thiele, K. Hoffman, R. Vetter, F. Marlow, S. Radaev, *Zeolites* **1997**, *19*, 190.
[38] S. H. Jhung, Y. S. Uh, H. Chon, *Appl. Catal.* **1990**, *62*, 61.
[39] B. M. Weckhuysen, I. P. Vannijvel, R. A. Schoonheydt, *Zeolites* **1995**, *15*, 482.
[40] M. S. Rigutto, H. vanBekkum, *J. Mol. Catal.* **1993**, *81*, 77.
[41] D. M. Hausen, *Am. Mineral.* **1962**, *47*, 637.
[42] B. I. Whittington, J. R. Anderson, *J. Phys. Chem.* **1993**, *97*, 1032.
[43] A. Miyamoto, Y. Iwamoto, H. Matsuda, T. Inui, in *Zeolites, Facts, Figures, Future* (Eds.: P. A. Jacobs, R. A. van Santen), Elsevier Science Publishers, B. V., Amsterdam, **1989**, p. 1233.
[44] C. A. Messina, B. M. Lok, E. M. Flanigen, *Eur. Pat.* **1984**, 131,946.
[45] G. Catana, J. Pelgrims, R. A. Schoonheydt, *Zeolites* **1995**, *15*, 475.
[46] J. W. Park, H. Chon, *J. Catal.* **1992**, *133*, 159.
[47] R. Hoppe, G. Schulz-Ekloff, S. Wohlrab, D. Wohrle, *Chem. Ing. Tech.* **1995**, *67*, 350.
[48] S. Prasad, R. F. Shinde, I. Balakrshnan, *Microporous Mater.* **1994**, *2*, 159.
[49] J. Das, V. V. Satyanaryana, D. K. Chakrabarty, S. N. Piramanayagam, S. N. Shringi, *J. Chem. Soc., Faraday Trans.* **1992**, *88*, 3255.
[50] D. Goldfarb, M. Bernardo, K. G. Strohmaier, D. E. W. Vaughan, H. Thomann, *J. Am. Chem. Soc.* **1994**, *116*, 6344.
[51] [51a] H. X. Li, J. A. Martens, P. A. Jacobs, S. Schubert, F. Schmidt, H. M. Ziethen, A. X. Trautwein, *Stud. Surf. Sci. Catal.* **1988**, *37*, 75. – [51b] S. Shubert, H. M. Ziethen, A. X. Trautwein, F. Schmidt, H. X. Li, J. A. Martens, P. A. Jacobs, in *Zeolites as Catalysts, Sorbents and Detergent Builders*, Elsevier Science Publishers, B. V., Amsterdam, **1989**, p. 735.
[52] J. Ma, B. Fan, R. Li, J. Cao, *Catal. Lett.* **1994**, *23*, 189.
[53] L. E. Iton, R. B. Beal, D. T. Hodul, *J. Mol. Catal.* **1983**, *21*, 151.
[54] D. H. Lin, G. Coudurier, J. C. Vedrine, *Stud. Surf. Sci. Catal.* **1989**, *49*, 227.
[55] A. Brückner, U. Lohse, H. Mehner, *Microporous Mesopor. Mater.* **1998**, *20*, 207.
[56] D. Goldfarb, *Zeolites* **1989**, *9*, 509.
[57] Z. Levi, A. M. Raitsimring, D. Goldfarb, *J. Phys. Chem.* **1991**, *95*, 7830.
[58] D. J. Parrillo, C. Pereira, G. T. Kokotailo, R. J. Gorte, *J. Catal.* **1992**, *138*, 377.
[59] A. Katzmarzyk, S. Ernst, J. Weitkamp, H. Knözinger, *Catal. Lett.* **1991**, *9*, 85.
[60] R. Roque-Malherbe, R. Lopez-Cordero, J. A. Gonzales-Morales, J. Onate-Martinez, M. Carreras-Gracial, *Zeolites* **1993**, *13*, 481.
[61] B. Z. Wan, K. Huang, *Appl. Catal.* **1991**, *73*, 113.
[62] U. Lohse, A. Brückner, E. Schreier, R. Bertram, J. Jänchen, R. Fricke, *Microporous Mater.* **1996**, *7*, 139.
[63] G. Brouet, X. Chen, C. W. Lee, L. Kevan, *J. Am. Chem. Soc.* **1992**, *114*, 3720.
[64] R. F. Mortlock, A. T. Bell, C. J. Radke, *J. Phys. Chem.* **1991**, *95*, 372.
[65] R. F. Mortlock, A. T. Bell, C. J. Radke, *J. Phys. Chem.* **1991**, *95*, 7847.
[66] J. Twu, P. K. Dutta, Kresge, C. T. *J. Phys. Chem.* **1991**, *95*, 5267.
[67] M. G. Uytterhoeven, W. A. VanKeyenberg, R. A. Schoonheydt, *Mat. Res. Soc. Symp. Proc.* **1991**, *233*, 57.
[68] M. G. Uytterhoeven, Schoonheydt, R. A. *Microporous Mater.* **1994**, *3*, 265.

[69] M. G. Uytterhoeven, R. A. Schoonheydt, *Proc. 9th Internat. Zeolite Conf.* (Eds.: R. von Ballmoos, J. B. Higgens, M. M. J. Treacy), Butterworth-Heinemann, Boston, **1993**, vol. 1, p. 329.
[70] G. Belussi, M. S. Rigutto, *Stud. Surf. Sci. Catal.* **1994**, *85*, 177.
[71] I. W. C. E. Arends, R. A. Sheldon, M. Wallau, U. Schuchardt, *Angew. Chem.* **1997**, *109*, 1190; *Angew. Chem. Int. Ed. Engl.* **1997**, *36*, 1144.
[72] D. L. Vanoppen, D. E. DeVos, M. J. Genet, P. G. Rouxhet, P. A. Jacobs, *Angew. Chem.* **1995**, *106*, 637; *Angew. Chem. Int. Ed. Engl.* **1995**, *34*, 560.
[73] M. J. Haanepen, A. M. Elemans-Mehring, J. H. C. vanHooff, *Appl. Catal. A: General* **1997**, *152*, 203.
[74] H. E. B. Lempers, R. A. Sheldon, *J. Catal.* **1998**, *175*, 62.
[75] L. H. Gielgens, I. H. E. Veenstra, V. Ponec, M. J. Haanepen, J. H. C. vanHooff, *Catal. Lett.* **1995**, *32*, 195.
[76] P. Concepcion, J. M. Lopez Nieto, J. Perez-Pariente, *J. Mol. Catal. A: Chemical* **1995**, *99*, 173.
[77] B.-Z. Wan, K. Huang, *Appl. Catal.* **1991**, *73*, 113.

Received August 5, 1998
[I98263]